Diamond Films and Technology
Vol. 6, No. 4 1996
MYU Tokyo

DFT 103

Continuous Diamond Fibres and Diamond Fibre-Reinforced Composites

Elizabeth D. Nicholson, Graham Meaden*, Elizabeth Kalaugher**, Peter G. Partridge*, Michael N. R. Ashfold, Paul W. May and Andrew Wisbey***

School of Chemistry, University of Bristol, Bristol BS8 1TS, U.K.
*Interface Analysis Centre, University of Bristol, Bristol BS2 8BS, U.K.
**Department of Aerospace Engineering, University of Bristol, Bristol BS8 1TR, U.K.
***DRA Farnborough, Farnborough, Hampshire GU14 6TD, U.K.

(Received 15 April 1996; accepted 24 June 1996)

Key words: diamond fibres, composites, laser processing

Diamond fibres, ~20–300 μm diameter and up to 150 μm long have been produced by chemical vapour deposition (CVD) on various metallic and ceramic core materials. Young's modulus values have been measured using several techniques including a resonance method and a tensile test. The composite fibres (core plus diamond coating) yield modulus values from ~700 to 900 GPa, depending on the deposition conditions and diamond volume fraction. These values are substantially greater than those for existing continuous fibre reinforcements (*e.g.*, SiC, modulus ~400 GPa) used in current commercial metal matrix composites. Titanium matrix composites containing diamond fibres have been produced, and both individual fibres and fibre-reinforced composites have been cut and profiled using pulsed laser radiation. A substantial increase in the effective diamond deposition rate, defined as diamond mass deposited per unit time, and a corresponding reduction in diamond fibre composite cost are predicted for deposition on multiple fibre arrays.

1. Introduction

Diamond's exceptional mechanical properties (high hardness, wear resistance, strength and Young's modulus) and superior thermal conductivity, chemical inertness and electrical insulating properties suggest a whole range of uses. The development of chemical vapour

deposition (CVD) techniques, that led to the production of diamond in film form,[1] has greatly extended this range. Deposition equipment currently available commercially can grow good-quality diamond at rates of over 10 μm h^{-1} on flat substrates of diameters over 15 cm. At least 13 companies worldwide are known to be selling CVD diamond products,[2] principally cutting tools, heatsinks, infrared (IR) windows and X-ray windows. Applications of CVD diamond films range from those that require a thin surface layer (0.5–20 μm) to those requiring thick (mm range) free-standing films (such as IR windows and domes).[3]

The production of diamond-coated fibres and wires and the potential for diamond fibre composites was reported in several papers in 1993.[4–7] In general, two approaches to their production have been considered. Firstly, the properties (*e.g.*, thermal and mechanical) of existing fibres can be improved by diamond coating. These fibres can be incorporated into composites, or used individually. Composites incorporating these fibres can then be produced with different properties by varying the morphology, composition and thickness of the diamond coating; and varying the volume fraction of the reinforcement.[8] An example of such a diamond fibre-reinforced composite is given in ref.9. To produce this composite, the diamond/SiC fibres were individually coated with Ti-alloy matrix material using physical vapour deposition, after which they were consolidated by hot vacuum pressing at 900°C.

Ting and Lake[10,11] considered diamond-coated fibres primarily for use in the area of electronics. They suggested that it may be possible to replace alumina and glass which are presently used as a reinforcement in epoxy for electrically insulating electronic packaging, with diamond-coated fibres. Diamond is a good electrical insulator and, together with its superior thermal conductivity, it would make a good packaging material, allowing a high power density per unit area in component design. They also suggested that conventional thermal management materials such as copper and aluminium could incorporate diamond fibres. This should lead to a substantial increase in their thermal conductivity (the thermal conductivity of diamond being around 5 times that of copper), reduce their thermal expansion coefficients to a value similar to that of silicon and gallium arsenide, and greatly reduce the mass of the thermal management material. Ting and Lake chose two carbon (graphite) cores with different microstructures on which growth of diamond was attempted. These were polyacrylonitrile (PAN) fibre, which showed a structure made up of a disordered arrangement of carbon ribbons, and vapour-grown carbon fibre (VGCF) which comprised carbon layers arranged in a tree ring pattern around a central region. These fibres, having diameters of 7 μm and 5 μm, respectively, were abraded prior to coating by microwave plasma enhanced CVD (MW-PECVD). The PAN fibres showed severe etching and only after a long deposition time (93 h) was there any sign of diamond formation. These diamond crystallites were less than 5 μm in size and sparsely distributed. Conversely, homogeneous coatings (up to ~5 μm thick) were formed on the VGCF. The diameter of the fibre core was observed to be somewhat reduced, suggesting some preferential etching of the more disordered structure prior to the diamond deposition.

In the second approach to the production of diamond-coated fibres and wires, the diamond coating is the matrix, and the core the reinforcement, thus producing a fibre-reinforced diamond matrix.[12,13] This should result in a substantial increase in the fracture toughness of diamond, which intrinsically is low (~5 MPa $m^{1/2}$). Drory and McClelland[12] produced a SiC-reinforced diamond matrix by closely spacing 100 μm-diameter SiC fibres,

50 mm in length, on a silicon wafer as a single unidirectional layer. MW-PECVD was used to deposit a CVD coating of thickness about 100 μm, at which point the fibres were turned over and deposition completed on the other side. Diamond film growth followed the outline of the fibres. A laser-cut cross section of the composite shows that the fibres are completely encapsulated in the diamond film. Drory and McClelland previously tested the viability of a reinforced diamond matrix by coating individual SiC fibres, thereby producing composite fibres 200 μm in diameter, 80 mm in length with a diamond volume fraction of 30–45%, and subjecting them to a tensile test. The composite fibres were observed to exhibit multiple matrix cracking and fibre pull out — a desirable type of fracture behaviour — and a fibre tensile strength of 1540 MPa.

Of primary interest in this paper is the use of diamond-coated fibres and wires as reinforcements in materials for the aerospace industry, particularly metal matrix composites (MMCs) reinforced with continuous unidirectional fibres.[14] Replacing existing reinforcements (*e.g.*, SiC, B and W) with diamond-coated fibres/wires would significantly increase the stiffness-to-weight ratio of the composite. Tungsten fibres have been used to reinforce superalloys for heat engines, and offer the potential for significantly higher component operating temperatures and thus improved heat engine performance. SiC fibres incorporated in Ti alloy, or Ti aluminide matrices are already in use in the aerospace industry. Carbon fibre, widely used in carbon fibre-reinforced polymer composites, is also being actively considered for some MMCs. Unidirectional composites offer outstanding unidirectional mechanical properties and, obviously, are particularly attractive for components that exploit such anisotropy. Reinforcement phases can also be in the form of particles, whiskers or chopped fibres. Candidate matrix materials include aluminium, magnesium, copper and titanium. Other applications presently under consideration include incorporation into grinding/polishing wheels and thermal conductors.

The mechanical properties of most interest for structural composites are Young's modulus and strength, both of individual reinforcement fibres and the resulting composite material. Due to the small size of the coated fibres (10–300 μm diameter) mechanical property measurement is difficult. Our present work is largely concentrated on the measurement of Young's modulus of individual fibres.

2. Manufacture of Diamond Fibres

2.1 *Solid fibres*

Diamond-coated fibres have been produced by both MW-PECVD and hot filament (HF) CVD, on a variety of substrate cores including SiC,[4,7,9,12,15] W,[7–9,15] Cu[7] and carbon[7,10,11] (Figs.1 and 2). The core material must be able to withstand high deposition temperatures (800–900°C), while remaining rigid and providing a surface suitable for diamond nucleation. Carbide-forming substrates are generally the most successful. Low thermal expansion is advantageous, as it reduces the probability of internal stress-induced film delamination on cooling from deposition temperature. Core materials with diameters as small as 5 μm have been used.

The substrate fibres and wires in this investigation W (25–125 μm diameter) and SiC (100 μm diameter), were diamond-coated by HFCVD using a purposely designed and built

(a)

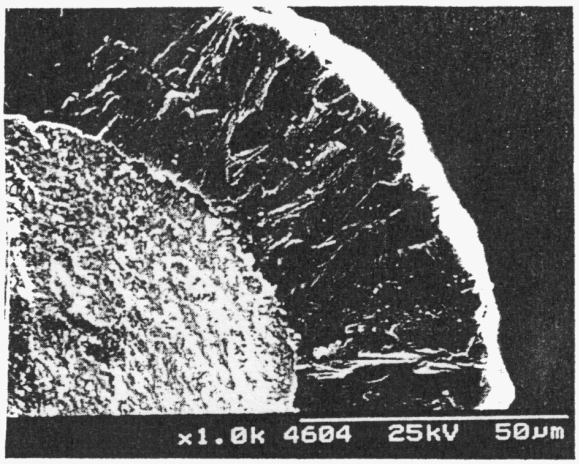

(b)

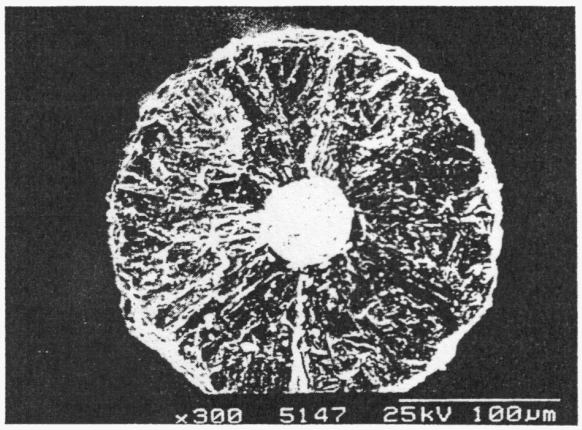

(c)

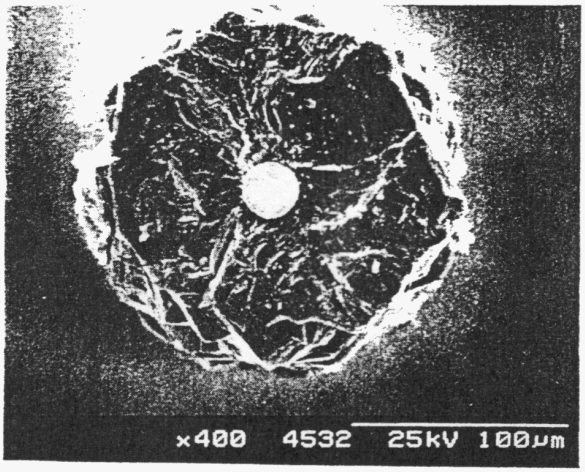

Fig. 1. Examples of diamond-coated W wires of various diameters produced by hot filament CVD: (a) 125 mm diameter wire with 55 mm diamond coating, (b) 50 mm wire with ~90 mm diamond, (c) 25 mm wire with ~71 mm diamond.

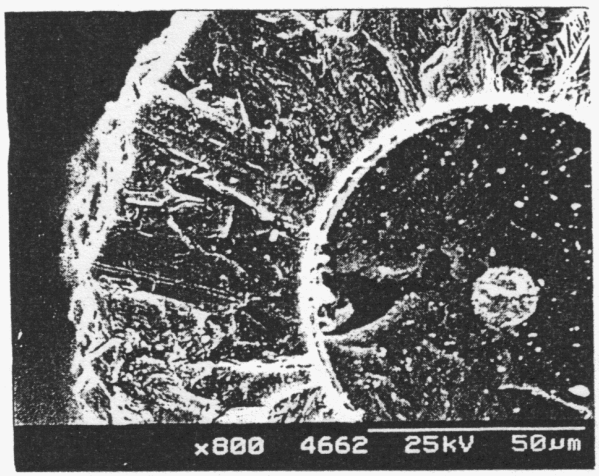

Fig. 2. A diamond-coated 'Sigma' SiC based fibre. The central core is W, coated with SiC, with a final outer coating of ~55 mm of diamond.

reactor.[16] Prior to deposition the substrates are abraded with diamond grit to enhance diamond nucleation. The sample wires (14 per run) surround a vertically held tantalum filament, at a distance of 5–6 mm from the filament. Samples with a working length of 100 – 120 mm are produced. The substrate temperature is determined by the filament temperature, which is measured using an optical pyrometer. Depending on the precise process conditions, we obtain deposition rates in the range of 0.5–1 µm h^{-1}. To date, deposition has been carried out for up to 105 h, which yielded film thicknesses such that on a 25-µm-diameter core the resulting fibres comprise > 95% diamond volume fraction. The standard deposition conditions are as follows: 20 Torr pressure, 0.5 – 1.25% CH_4 in H_2, filament temperature 2150–2200°C, and gas flow rate 200 sccm. Smaller diameter (10–15 µm) cores have also been coated,[17] as shown in Fig. 3; their lengths however are restricted to 10–20 mm.

2.2 *Hollow fibres*

Several methods of producing hollow diamond fibres have been suggested.[6,7,18] Tubes of 5–6 mm length can be produced by etching out the core of a diamond-coated metal wire (Fig. 4). For tungsten cores, a hot hydrogen peroxide etch was used.[6] This technique is not suitable for long lengths and cores of small diameter due to the difficulties of transporting the etch to the reaction site and removing the waste products, although there is potential for electrochemical means of overcoming such problems. Longer hollow fibres can be produced by diamond coating a finely wound coil of W wire. A 20 µm-diameter W wire was wound around a stainless steel former (200 µm diameter) with a suitable small pitch to produce such coils.[18] As Fig. 5 shows, upon diamond coating each turn of the coil becomes attached to its neighbour by the growing film and eventually closes up to form a tube, encapsulating the W wire. We are presently able to produce such tubes with lengths > 20 mm, though maintaining their straightness during deposition remains a major difficulty.

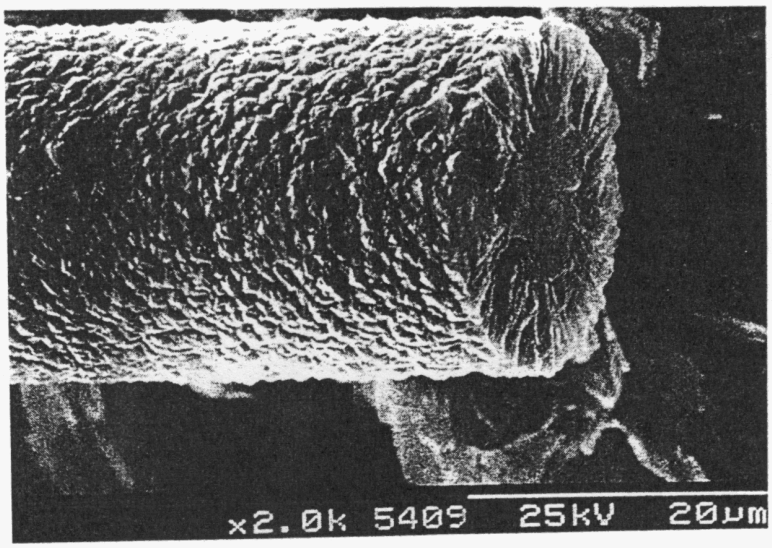

Fig. 3. A 10-15 mm-diameter SiC-based Tyranno fibre coated with ~6 mm of diamond.

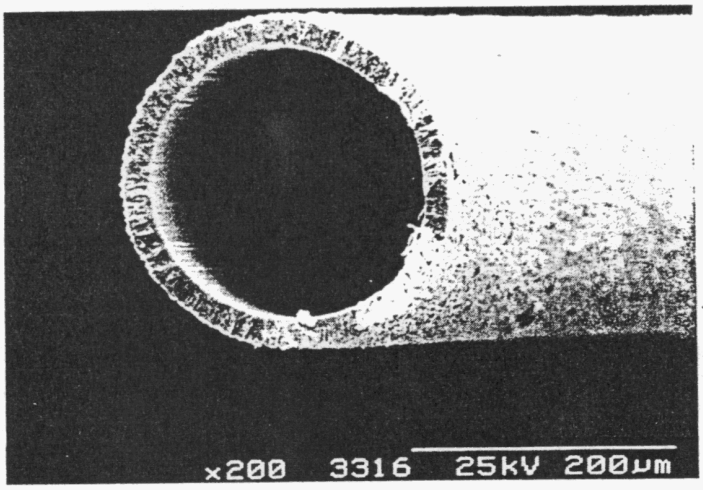

Fig. 4. A hollow diamond fibre, or tube, produced by etching the W core from inside a diamond-coated wire using hot hydrogen peroxide. The tube length is around 5 mm.

2.3 *Fibre arrays*

Parallel arrays of fibres and fine fibre meshes have been diamond-coated.[12,13,19] Figure 6 shows consolidation of alumina-based Nextel fibres by diamond coating. These fibres (~10 µm in diameter), originally part of a tow, were thinned out to produce almost a monolayer prior to coating. On coating, the diamond film grew, connecting each fibre to its neighbour along its length.

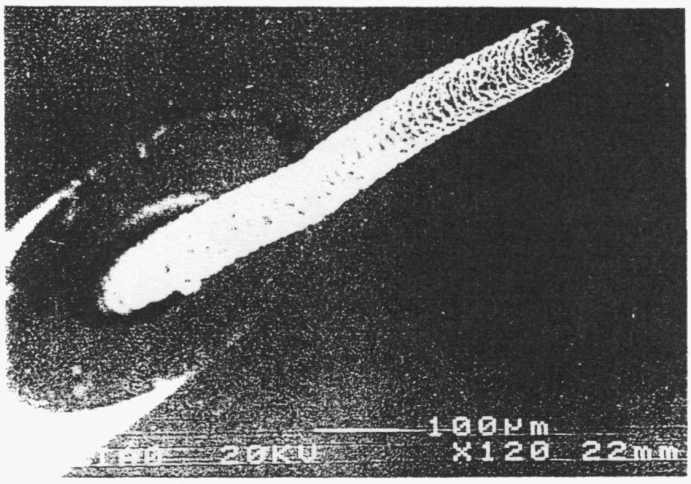

Fig. 5. A diamond tube made by coating a W helix. As the coating increases in size, eventually the coating on neighbouring coils meets and fuses to make a tube. In order to better illustrate the scale, the diamond tube is shown here inside the end of a fine hypodermic needle.

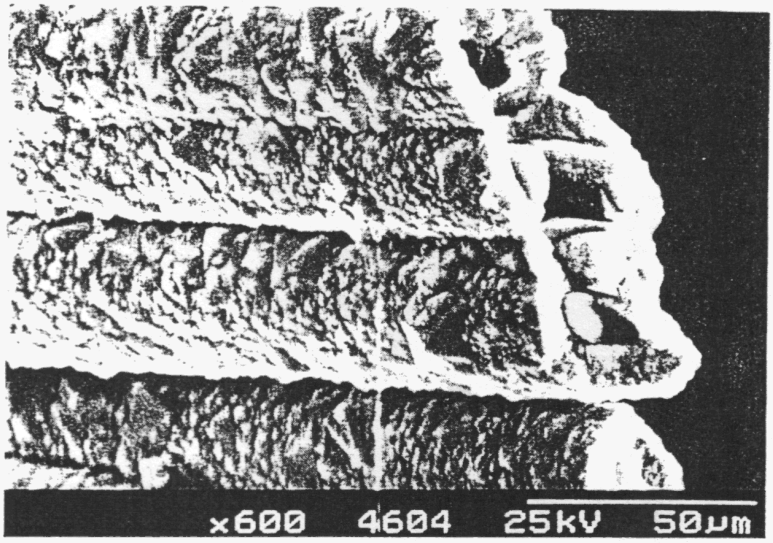

Fig. 6. An array of alumina-based Nextel fibres that have fused along their length during deposition to produce a solid sheet.

A 2-dimensional W mesh (wire diameter 20 µm, with ~0.5 mm wire separation) has also been coated.[13,19] To encourage nucleation the mesh was doused in a diamond powder/methanol mixture prior to CVD. Diamond was deposited under typical conditions, for 70 h, producing a film of 30–40 µm thickness (corresponding to a growth rate of ~0.5 mm h^{-1}). SEM observations of the coated mesh reveal good nucleation and coverage by diamond (Fig.

7(a)). At cross-over points the W wires became embedded in diamond forming a ridged fibre array (Fig. 7(b)). Using a finer mesh and/or longer deposition times, it should be possible to fill the mesh to produce a reinforced composite sheet. Production of 3-dimensional arrays by a similar route was proposed.[19]

(a)

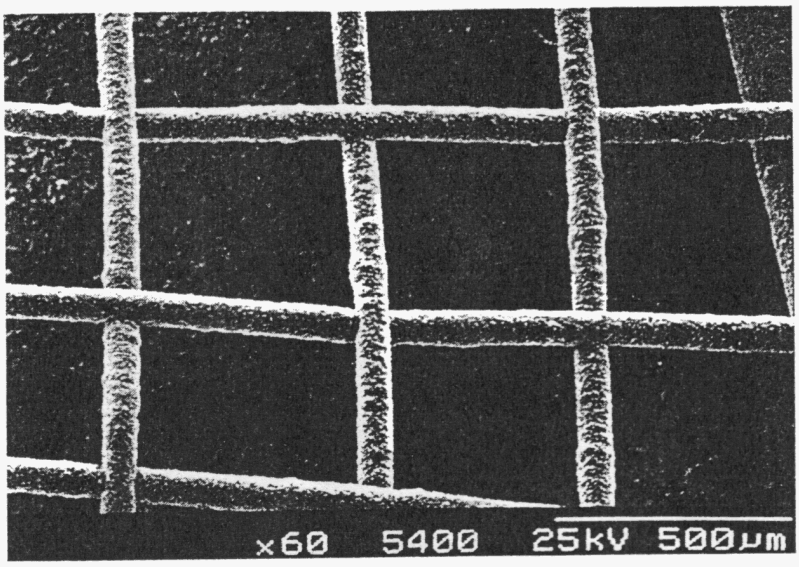

(b)

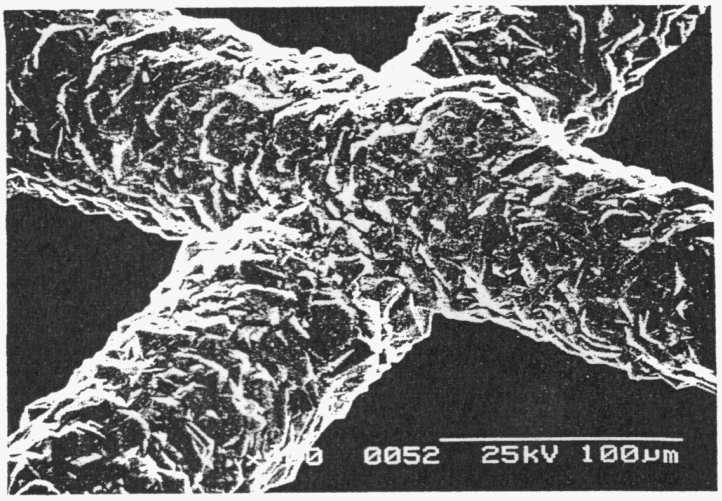

Fig. 7. (a) Diamond-coated W wire mesh. (b) Close up, showing that the diamond coating has fused the W wires together at the joints and thickened the entire structure, creating a rigid 2-D frame.

3. Young's Modulus of Diamond Fibres

Young's modulus is one of the most important mechanical properties when considering diamond-coated fibres for applications such as MMCs. We have developed a resonance method and a tensile test specifically for this purpose.[13,20] The basis of resonance methods[21,22] is the measurement of the natural or resonant frequency of vibration of a sample which, together with knowledge of the sample density and dimensions, yields the Young's modulus. The most accurate resonance methods impose minimum constraint on the sample. Resonance techniques applied to fibres have concentrated on methods where the fibre is clamped rigidly at one end and excited into vibration. Such techniques introduce large length errors. A more accurate method involves the sample being simply supported at nodes for fundamental flexural vibration (0.224 of the length from each end). This technique, previously applied to much larger samples,[23,24] has been miniaturised and optimised for the samples under test. Sample excitation is achieved using an audio speaker and resonance is detected by laser interferometry.[15] The resonance frequency is related to Young's modulus by a standard formula.[20–22] The fibres under test consisted of a 50 μm W core coated with ~85 μm diamond, producing fibres which were predominantly (~95%) diamond. An average fibre modulus of 874 ± 45 GPa (for a 95% confidence interval) was calculated, which was more than a factor of two greater than that for SiC fibre (400 GPa). If these fibres were coated with 10 μm of Ti alloy (modulus 115 GPa) and consolidated into a composite, the resulting composite sample would comprise 84% diamond. Using the rule of mixtures we can predict a composite modulus of ~750 GPa, which is more than 3.5 times that of current Ti-alloy/SiC fibre composites (~206 GPa) with about 30% fibre volume fraction.

The tensile test is the most widely used technique for measuring the modulus of stiff fibres. This involves measuring the load-elongation behaviour of samples of known cross-sectional area.[23,24] The tensile test can measure both the stiffness and the fracture stress of fibres. In general, difficulties have been experienced in gripping the sample successfully and measuring the small strains experienced by very stiff fibres. Due to the very small strain-to-failure of diamond-coated fibres, conventional methods of correcting for the compliance of the load cell are inadequate. Thus we are investigating a direct method for measuring the fibre.[25] The fibres are mounted on test cards using epoxy resin producing a gauge length of ~70 mm. A 14 μm-diameter marker fibre is attached at each end of the fibre using cyanoacrylate. The card is gripped in a Hounsfield H5000M tensile tester, with a 500 N load cell. After the sides of the test cards are cut, the lower grip of the tensile tester is moved downwards at 0.5 mm min^{-1} until the fibre breaks. The motion of each marker fibre shadow is tracked using a CCD linear array camera. The relative motion of the two markers during loading gives the fibre extension, without any contribution from the machine compliance, or slip of the fibre through the epoxy resin. The original length of the fibre can be calculated from the initial marker positions. Young's modulus can be calculated from the fracture stress and strain to failure, or from the slope of a stress-strain curve. Tensile testing produces modulus values for the composite fibre. The average modulus for seven fibres, each consisting of a 125 μm tungsten core coated with 40 μm of diamond (~62% diamond volume fraction), tested to date is 761 ± 100 GPa (for a 95% confidence interval). Using the rule of mixtures, the average modulus of the diamond coating from this fibre modulus can be calculated to be about 970 GPa.

The total experimental error for the resonance test and the tensile test is calculated to be 10% and 15%, respectively. As different samples were used in each test the results cannot be compared directly. However the fibres with higher diamond volume fraction used in the resonance test can be expected, and indeed have been found, to give higher modulus values than those tested by the tensile test.

4. Manufacture of Continuous Diamond Fibre Composites

Diamond fibre composites have been manufactured using a matrix-coated fibre method.[14] This involved barrier layers and physical vapour deposition (electron beam or sputter coating) of a matrix onto the fibres (Fig. 8). The aligned diamond fibres were then stacked and vacuum hot pressed either unidirectionally or isostatically (HIPed) to consolidate the composite. The inter-fibre spacing was dictated by the thickness of the matrix material; fibre volume fractions up to 80% are achievable.[14] Figure 9 shows an example of a titanium-diamond fibre composite, produced by embedding sputter-coated diamond fibres in Ti-6Al-4V alloy and HIPing at 900°C.

5. Laser Cutting of Diamond Fibres and Composites

Figure 10 serves to illustrate the fact that mechanical cutting of diamond-coated fibres and diamond fibre-reinforced composites without damage is extremely difficult owing to the extreme hardness and low ductility of diamond. Compared with alternative methods, laser processing is particularly attractive for cutting, polishing and profiling diamond fibres and, together with diamond machining, is the preferred method for preparing microsections and test pieces.

Two different pulsed (10 Hz) Nd-YAG lasers, one equipped with unstable resonator optics (yielding a 'ring doughnut' output beam profile), the other with more conventional 'filled-in' beam optics, were used in these preliminary studies. In both cases their output was

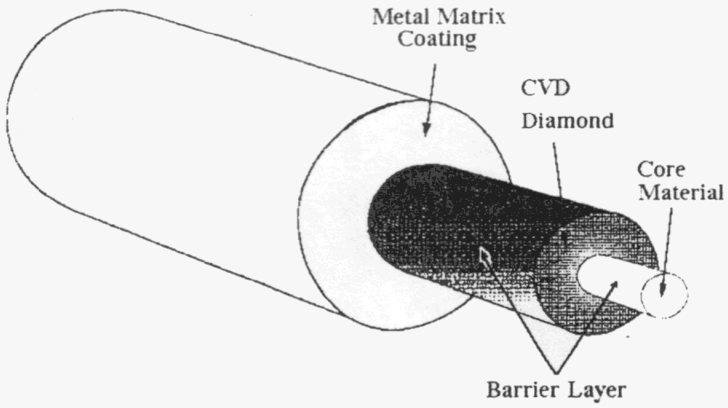

Fig. 8. Schematic diagram of diamond-coated wire before incorporation into a metal matrix composite. The diamond-coated wire is sputter-coated with typically 10 mm of the matrix metal (*e.g.* Ti alloy) before HIPing.

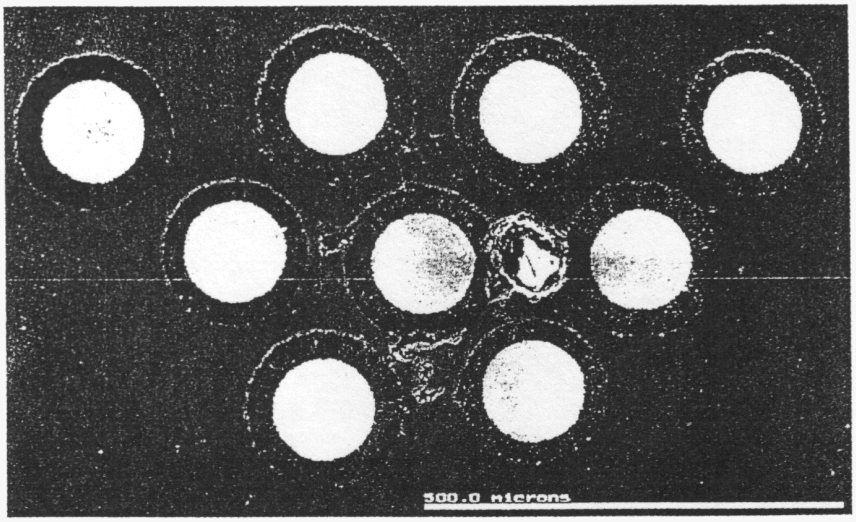

Fig. 9. SEM image of Ti-6Al-4V / W-cored diamond fibre composite polished section normal to fibre axis.

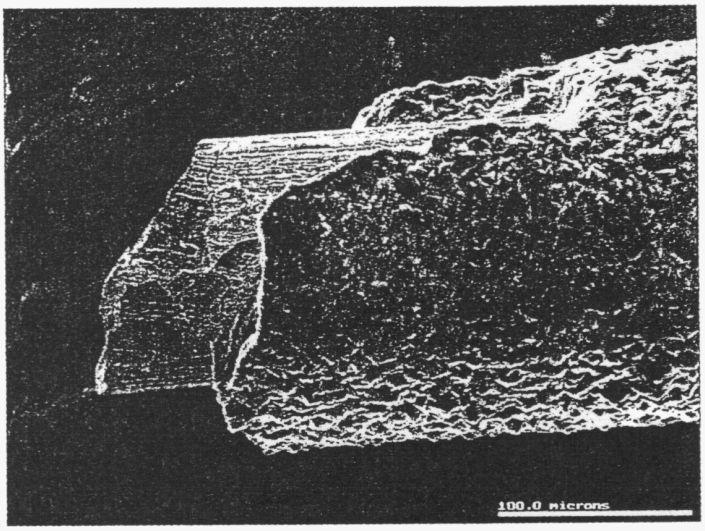

Fig. 10. SEM image of a mechanically cut diamond fibre. The cut is ragged and the coating has cracked and partially delaminated for over 100 mm from the cut.

focused using a cylindrical lens to produce a line (rather than a spot) focus across the fibre, of width down to 50 mm. Parameters explored thus far include wavelength (1064 nm and 355 nm), pulse energy, and the duration of exposure to radiation (i.e., number of pulses). Individual fibres were held vertically and then displaced in the vertical direction in steps, between cuts, and irradiated from one side under various conditions. All laser processing described here was carried out in air.

5.1 *Laser profiling of diamond fibres*

An SEM image of a diamond-coated fibre after localised ablations is shown in Fig. 11. The areas of the surface at 'A' are unirradiated, and appear bright due to the enhanced electron emission characteristics of CVD diamond. The irradiated upper surface 'B', between the bright bands, appears darker. Micro-Raman spectra (Fig. 12) taken from the irradiated areas show an increase in the graphitic content of the film surface, but also indicate the presence of diamond. Auger analysis (Fig. 13) shows areas like 'A' to be diamond, and areas like 'B' to be graphite. Since the sampling depth of the micro-Raman technique is of the order of 1 μm, whilst that for the Auger analysis is about 10 nm, we conclude that surface graphitisation has occurred to a depth of < 1 μm. Unfortunately, Auger depth profiling is not possible on a diamond sample due to the graphitisation caused by the ion beam.[26,27] We note, however, that Ralchenko *et al.*[28] have reported that Raman spectra of similar graphitised diamond surfaces after exposure to a hydrogen plasma show no evidence of graphitic carbon formation, again implying that the bulk of the CVD diamond is largely unaffected by the laser ablation treatment.

Mechanically cut fibres show cracks in the W core as well as cracking and spalling of the diamond coating (Fig. 10). This damage is absent in a fibre cut with a Nd-YAG laser operating at a wavelength of 355 nm (Fig. 14(a)). The cut surface is planar and very smooth across both the diamond and the core (Fig. 14(b)). However, further SEM investigation shows that particles of condensed tungsten are deposited around the ablated W core and on the fibre surface, *e.g.*, at 'A' in Fig. 14(a).

Partial cuts can be formed by using low power or short exposure times. A variety of cut profiles can be produced, depending on the laser optics and processing conditions. Figures 15(a) – (c) illustrate that smooth-sided 'slots' (short time, well-focused 'doughnut shape' beam), wide V notches (Gaussian beam) or even irregular series of narrow sharp peaks (long

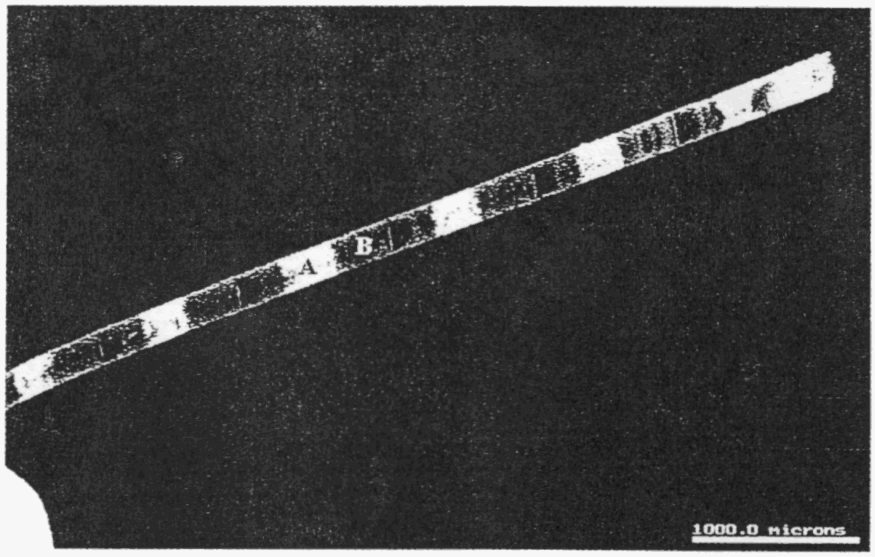

Fig. 11. Low-magnification secondary electron image of a diamond fibre showing laser irradiated area at 'B' and unirradiated area at 'A'.

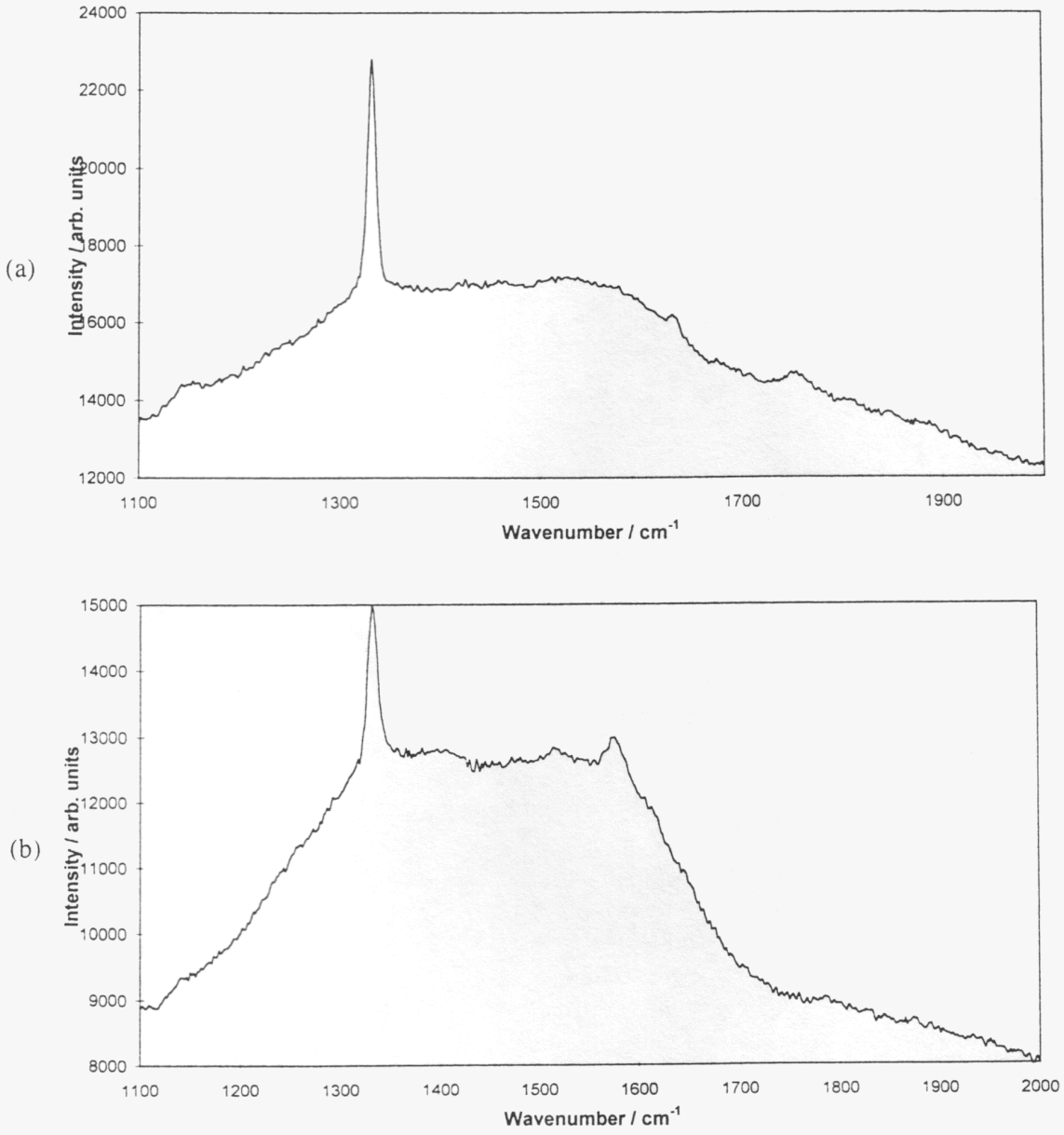

Fig. 12. Laser Raman spectra of diamond fibre showing, (a) before laser treatment, the sharp peak at 1332 cm^{-1} due to diamond, and (b) after laser ablation, an additional broad peak around 1600 cm^{-1} attributed to graphitic carbon.

time, imperfectly focused 'doughnut shape' beam) can all be obtained using the 355 nm output from commercial Nd-YAG lasers.

Relative ablation rates are revealed by partially cut sections. Consider, for example, the partial cut through a diamond-coated SiC fibre shown in Fig. 16. The ablation front 'ABCD' shows a greater depth of cut at the SiC core 'BC', indicating a faster ablation rate (at 355 nm)

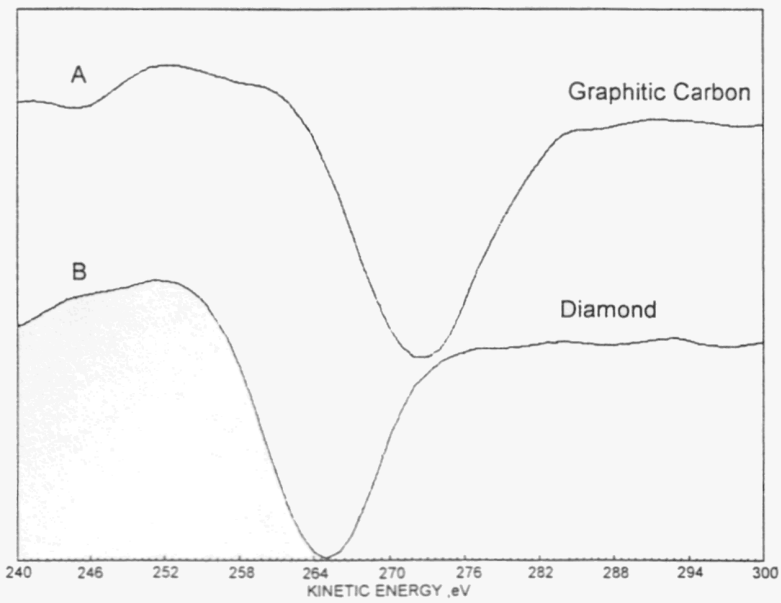

Fig. 13. Auger spectra taken from areas 'A' and 'B' on Fig. 11 showing characteristic carbon *KLL* profiles for diamond and graphite, respectively [26].

for SiC compared with CVD diamond. Conversely, we find that the W core in a diamond-coated W wire ablates at a slower rate than the diamond (Fig. 15(c)). Figure 17 shows a plot of measured depth of laser cut in CVD diamond against time; the slope translates to an ablation rate of 0.045 μm shot^{-1} (0.45 μm s^{-1}) at an estimated fluence of 10 J cm^{-2}. In agreement with many previous studies of material ablations we find UV (355 nm) radiation to be one or more orders of magnitude more efficient than the 1064 nm fundamental wavelength of the Nd-YAG laser at ablating both the CVD diamond and the SiC (or W) core, and that there is a threshold intensity (estimated at about 2×10^8 W cm^{-2} at 355 nm) below which no material ablation occurs. Similar trends have been reported at various excimer laser wavelengths, and the ablation rate correlated with the absorption coefficient of the sample.[28]

Laser ablation appears to progressively smooth individual diamond facets until very smooth areas are produced across many grain boundaries in the diamond (Figs. 18(a) and (b)). Smoothing of CVD diamond deposits has been reported by several workers.[29–31] The ablation rate and extent of smoothing have been shown to depend on the angle of incidence, a.[31] For example, using an excimer laser on a flat deposit the surface roughness was found to decrease from $R_a = 0.65 - 0.8$ μm for the as-deposited diamond to 0.38 μm ($a = 0°$) and to 0.15 μm ($a = 75° - 80°$), with a corresponding decrease in the etching depth.[32] Obviously such variations will be relevant to laser smoothing of diamond-coated fibres, for which the angle of incidence of the beam (relative to the surface normal) necessarily varies from 90° (at the centre of the fibre) to 0° at the edge. As the grain size of CVD diamond increases with thickness, this will decrease the absorption coefficient,[30] thus we can expect the ablation rate of our fibres to depend on film thickness also.

(a)

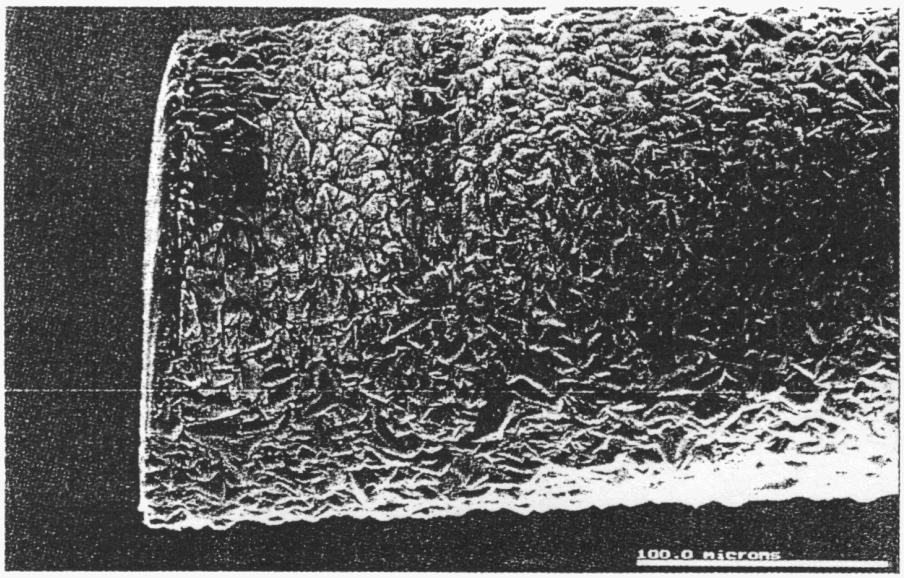

(b)

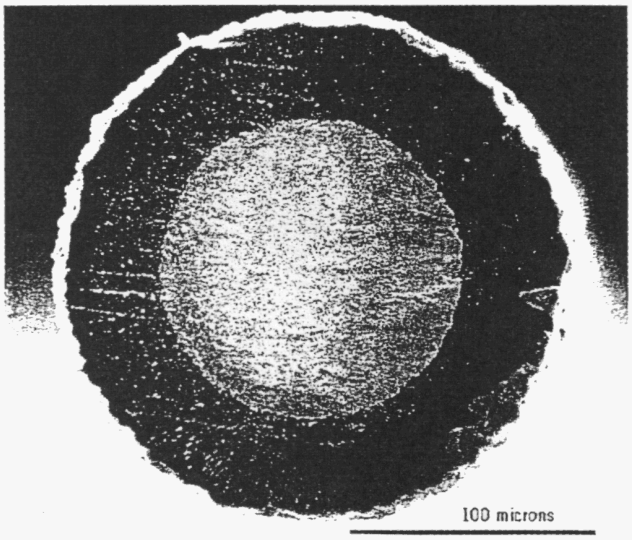

Fig. 14. SEM of laser-cut diamond fibres (a) side view and (b) normal to fibre axis. The cut is very smooth across both the diamond and the W, and there is no evidence of cracking or spalling of the coating. Particles of condensed tungsten are, however, deposited around the ablated W core and on the fibre surface (marked as 'A').

None of the lasers used in this work had the optimal spatial or temporal homogeneity required for fibre processing. Studies of cut depth as a function of laser fluence were also complicated by the fact that the spatial distribution of the beam profile is dependent on the

(a)

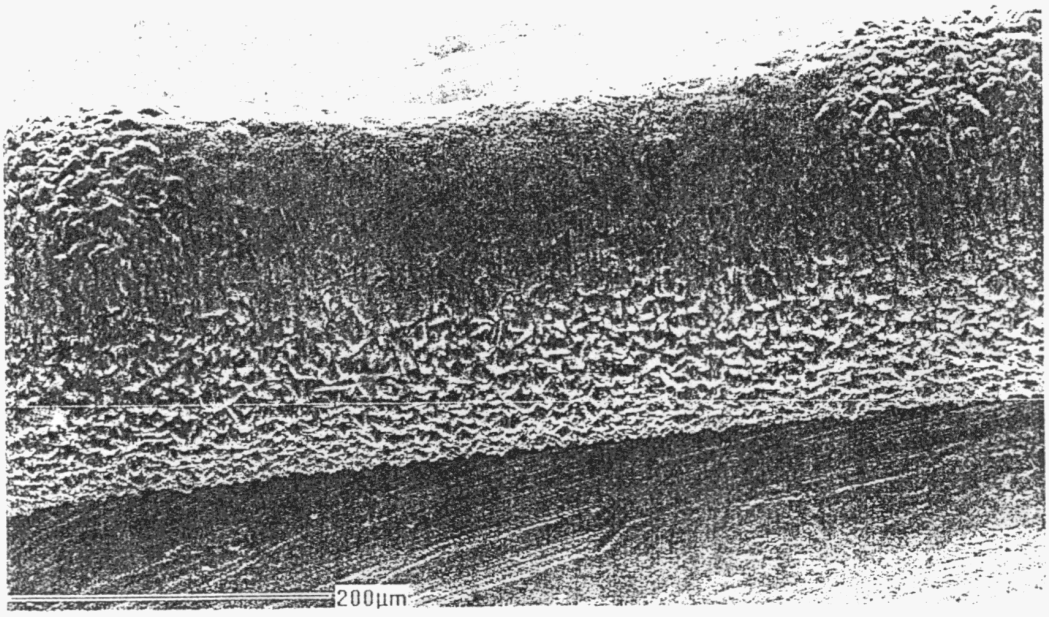

(b)

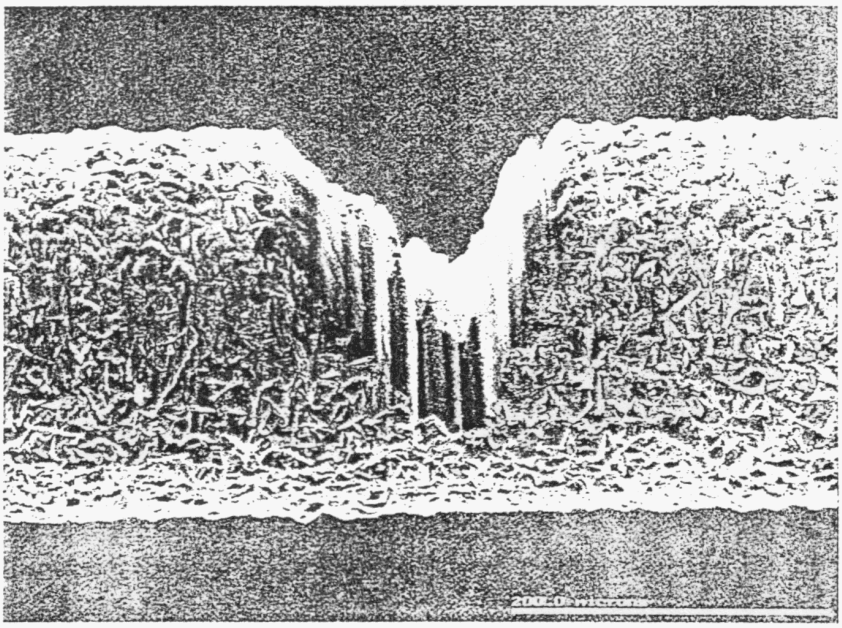

Fig. 15. Partially laser-cut diamond fibres. (a) short duration cut demonstrating polishing effect and (b) longer duration cut with 'filled-in' beam optics.

(c)

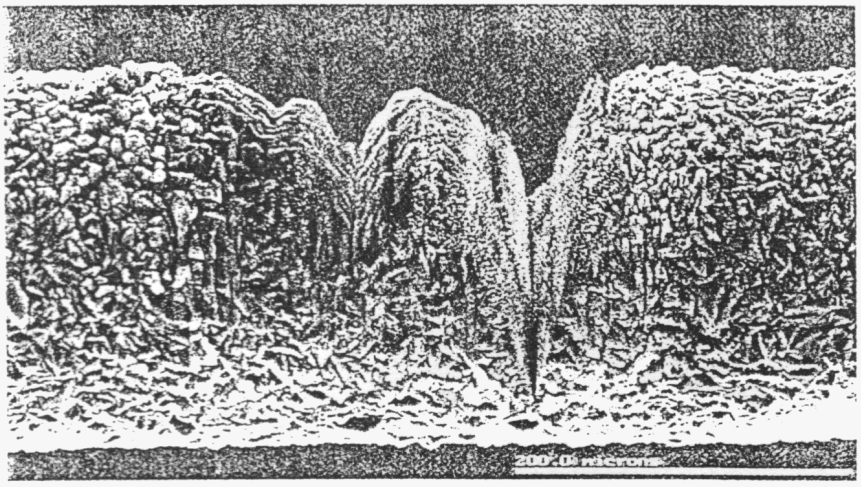

Fig. 15. Partially laser-cut diamond fibres. (c) longer duration cut with unstable resonator 'doughnut' shaped beam.

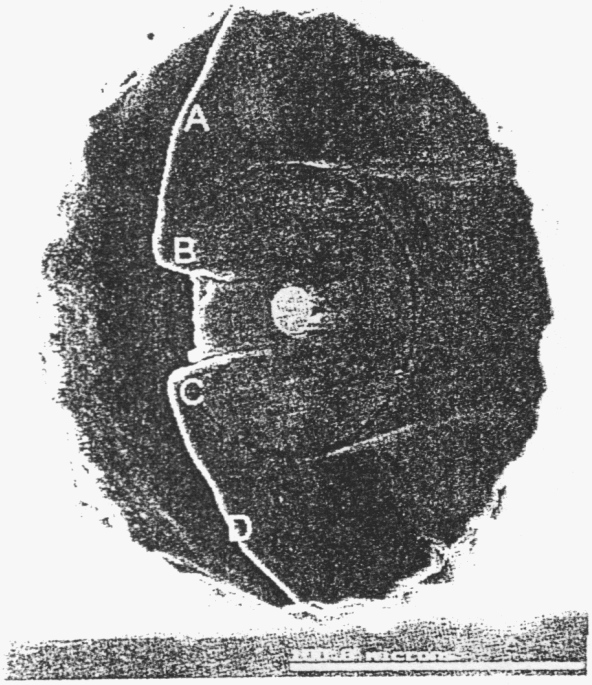

Fig. 16. Plane normal to diamond-coated SiC fibre axis showing a partial laser cut. Area 'BC' shows where the cut has penetrated the SiC core and the cutting rate has increased relative to that of diamond.

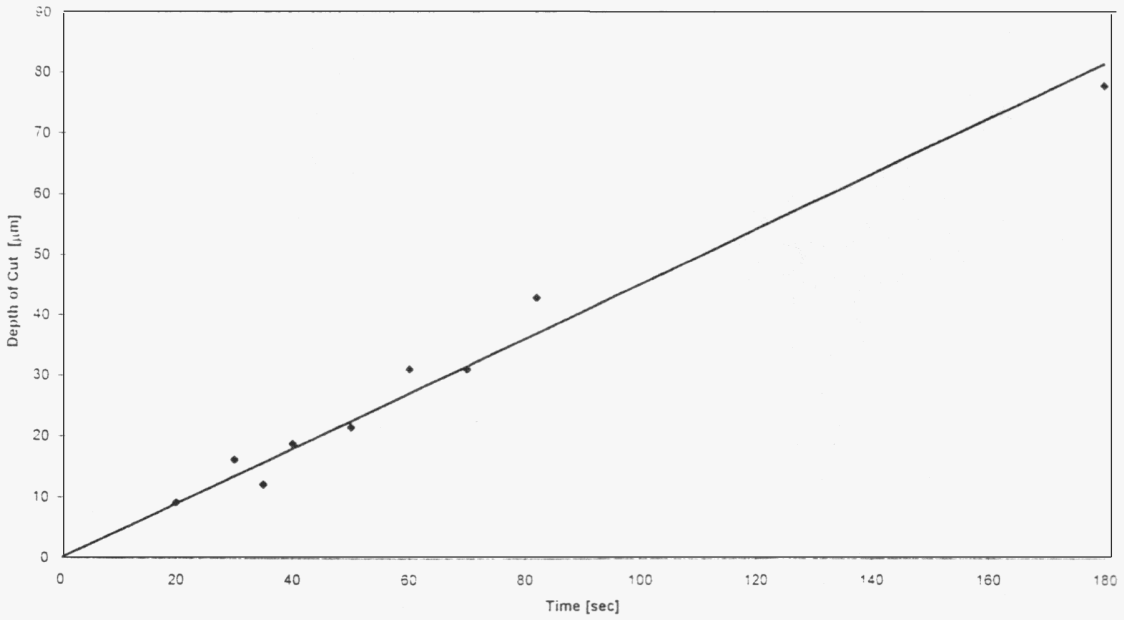

Fig. 17. Plot of depth of laser cuts in CVD diamond against time for an estimated laser fluence of 10 J cm $^{-2}$.

laser output energy. Faster cutting rates and more uniform cut profiles are now being achieved using an excimer laser.

5.2 *Laser cutting of diamond fibre-reinforced Ti-alloy composite*

Cutting MMCs mechanically causes severe abrasive damage, as can be seen from a close up of the rough diamond surface (Fig. 19) that resulted from mechanical cutting of the composite shown in Fig. 9. As before, a better method is to use lasers. A polished section normal to the fibre axis in a Ti-6Al-4V / W-cored diamond fibre composite is shown in Fig. 20. The corresponding surface of an unpolished laser cut section through the same composite is shown in Fig. 20(a). Although the laser cut surface is not planar on a macroscopic scale, locally the surface is smooth, for example in the Ti-alloy matrix at 'X' and across the Ti-diamond-W phases ('AB' in Fig. 20(b)). The smooth surface and lack of surface damage are revealed by the sharp edges around the residual pore present in the Ti-alloy matrix at 'C'. The cut areas away from the ablation front become coated with a Ti deposit as shown by 'D' in Fig. 20(b). This and similar deposits can be removed by very gently polishing the cut surface with 1 μm diamond powder.

Laser processing has a clear advantage over mechanical methods for cutting diamond fibres without damage. The present results show that diamond fibres embedded in a reactive metal such as Ti alloy may also be cut to a smoother cut diamond surface finish than is obtained with a mechanical method. Lasers may also be used for profiling or smoothing the fibre surface. This could allow greater flexibility in the design of both solid and hollow diamond fibres and composites based on the fibres.

(a)

(b)

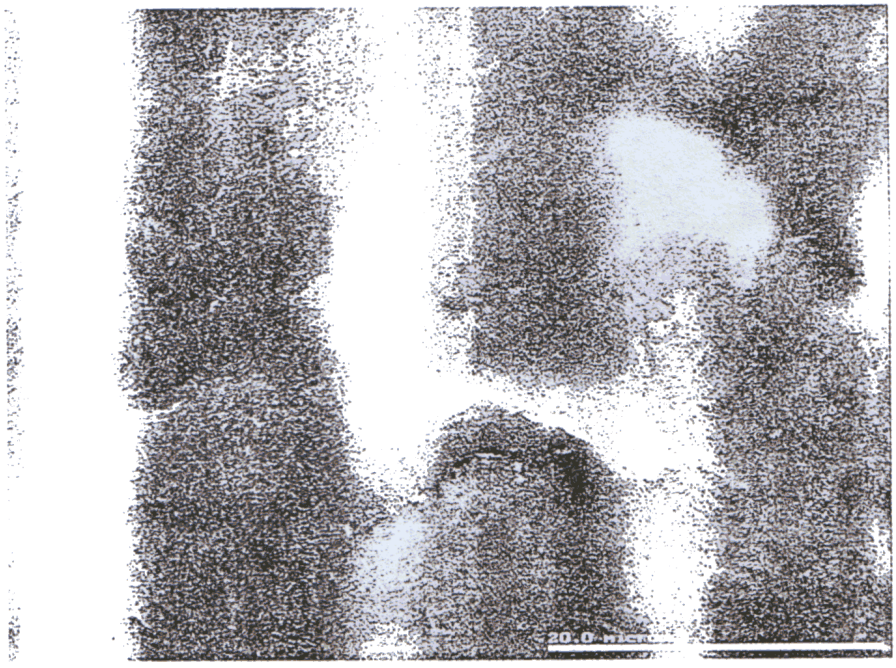

Fig. 18. Smoothing effect of laser irradiation on surface diamond facets. (a) Initial smoothing and (b) almost complete smoothing.

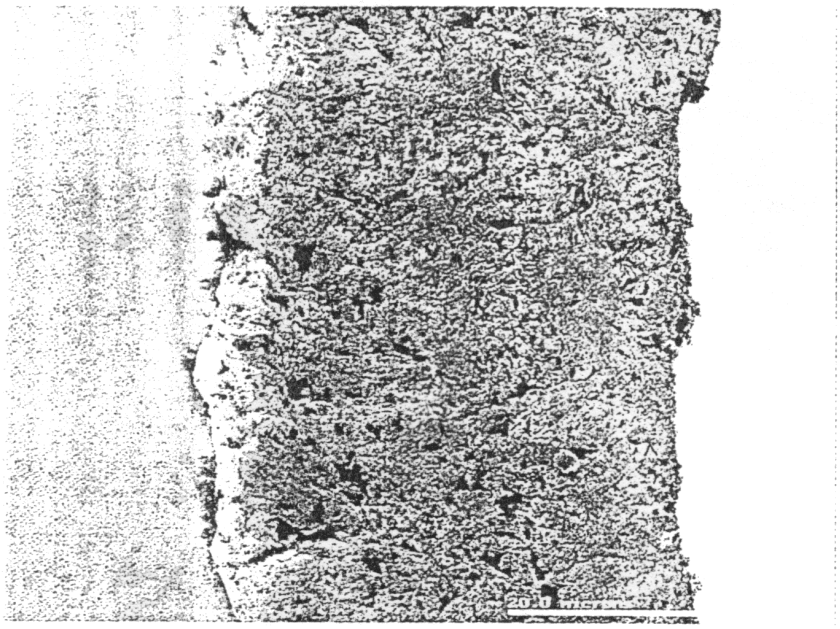

Fig. 19. Rough, abraded diamond surface in the mechanically cut polished section shown in Fig. 9.

6. Effective Deposition Rate of Diamond

The effective chemical vapour deposition rate of diamond, defined as the total thickness of diamond or as the mass of diamond deposited per unit time, may be increased by orders of magnitude by increasing the substrate area per unit volume. To obtain these high deposition rates, novel substrate designs have been proposed that exploit 3-dimensional arrays of small-diameter wires or fibres.[19]

The diamond deposition rate on free-standing substrates with flat and cylindrical surfaces is shown schematically in Fig. 21. If x_1 is the increase in diamond deposit thickness measured normal to the substrate surface after time t (Fig. 21(a)), the conventional deposition rate is given by $R = x_1/t$. It is sometimes convenient to consider an effective diamond deposition rate, R_{eff}, defined as the rate of increase in the total thickness of diamond in a particular direction. In the Y direction in Fig. 21, R_{eff} is x_1/t for one flat surface (Fig. 21(a)), $2x_1/t$ for two flat surfaces (Fig. 21(b)) and $2x_1/t$ along the diametral direction of a cylinder (Fig. 21(c)).

The volume (or mass) of diamond deposited per unit time is also used as a measure of the deposition rate. The specimens shown in Fig. 20 all have the same projected area, $L_1 \times L_2$. If N is the number of specimens coated simultaneously in each case, the volume of diamond deposited is:

on multiple single flat surfaces	$V_1 = N x_1 L_1 L_2$	(Fig. 21(a))
on multiple double flat surfaces	$V_2 = 2N x_1 L_1 L_2$	(Fig. 21(b))
on multiple cylindrical surfaces	$V_3 = N\pi (L_1 x_1 + x_1^2) L_2$	(Fig. 21(c))

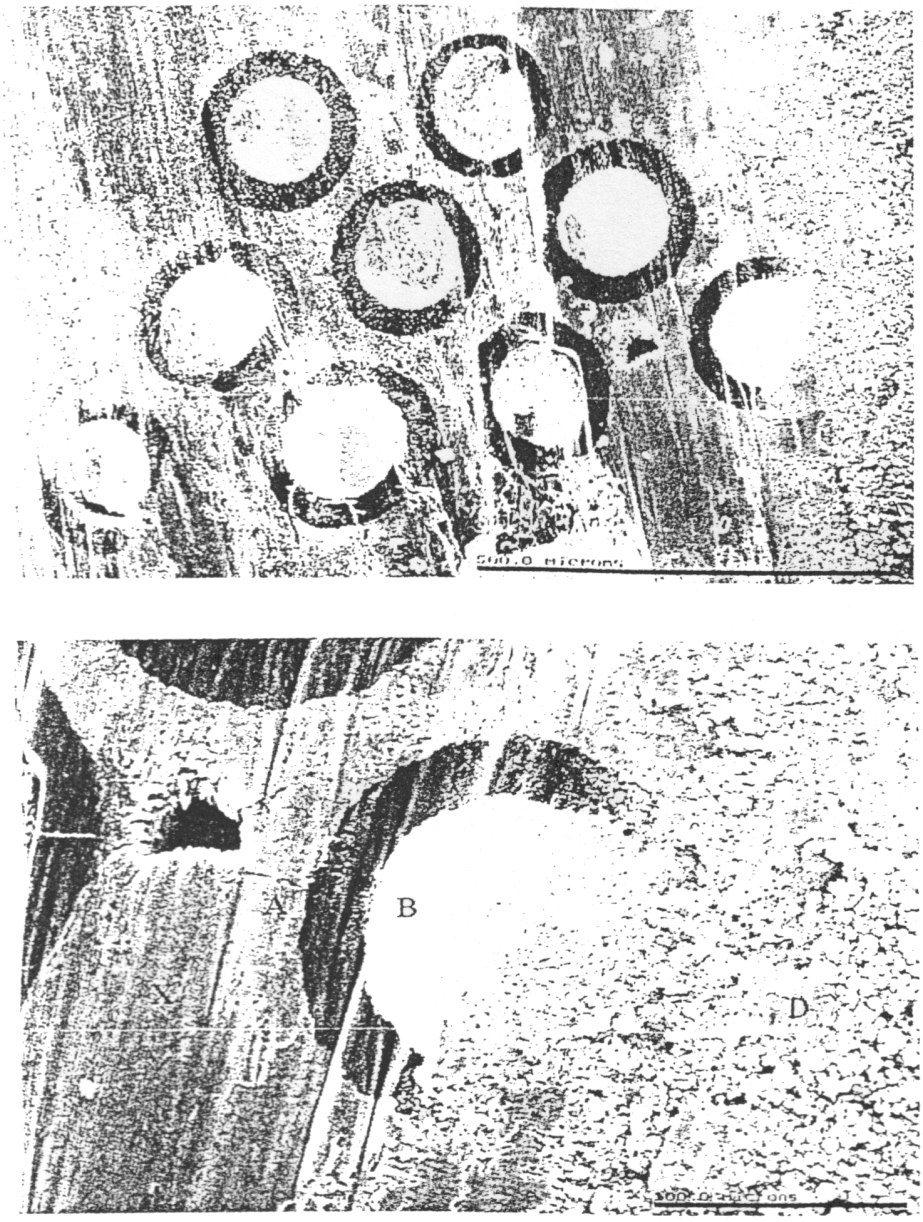

Fig. 20. (a) Laser-cut section of the composite shown in Fig. 9. (b) Smooth areas extending across the Ti-diamond-W phases 'AB', and in the Ti-alloy matrix itself at 'X'. A residual pore in the Ti-alloy matrix at 'C' can also be seen. Ti from the ablation front has been redeposited at 'D'.

For typical x_1/L_1 values of 0.10 – 10, the corresponding mass or volume ratios are $V_1:V_2:V_3 = 1:2:3.5-35$). Thus in practice the mass of diamond deposited per unit time is proportional to the total substrate area and may be one order of magnitude greater for cylindrical surfaces than for a single flat surface.

Since large numbers of fibres and hence a large surface may be coated simultaneously,

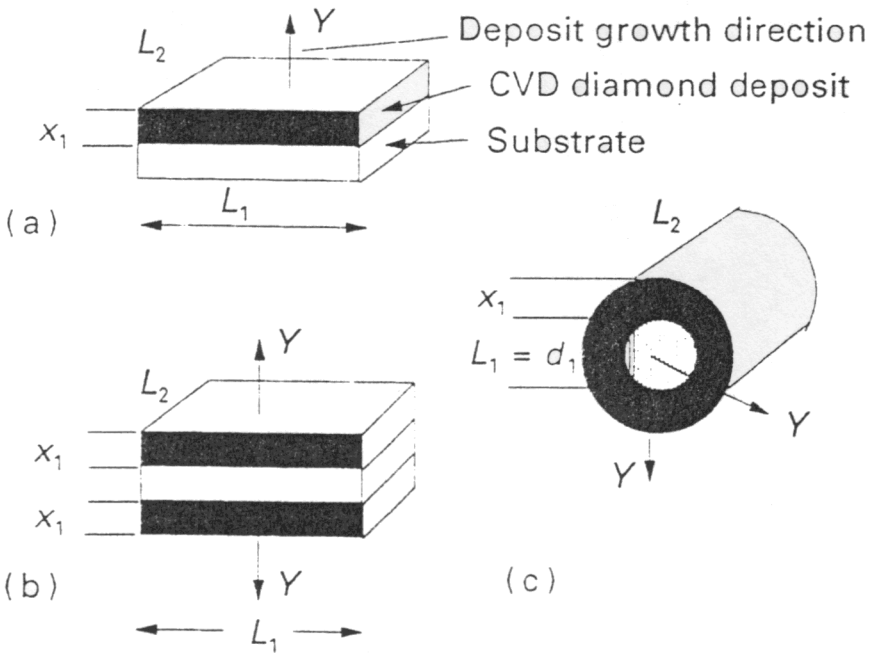

Fig. 21. Schematic diagram showing diamond deposition onto various surfaces. (a) Planar one sided, (b) planar two sided, and (c) cylindrical.

the effective deposition rates can be very high. Consider a hypothetical and extreme example using wires or fibres of $d_1 = 20$ μm, coated with diamond to a thickness $x = 50$ μm, to give a fibre with an outside diameter of 0.12 mm and a diamond volume fraction of 97%. A 3-D fibre array (Fig. 22) of 100×100 fibres of, say, 1 m length (length limited only by the reactor size) could be coated in $t = 50$ h at an effective rate $10^2/50 = 200$ m h^{-1}. This might be compared with the deposition of 50 μm-thick diamond onto individual 10 m-long wires in 50 h at a rate of $10/50 = 0.2$ m h^{-1}. This simple comparison indicates that the array offers a possibility of coating fibres 3 orders of magnitude faster than a single fibre technique. Alternatively, deposition may be continued on this array of fibres until $t = t_c$ to manufacture a solid bar with a 12 mm × 12 mm cross section and any length. This 12 mm thickness would consist of 10 mm thickness of diamond and would be obtained in 50 h, giving an effective deposition rate of 200 μm h^{-1}. This rate is some 200 times the rate for hot filament CVD growth, 25 times that for combustion flame growth and some 8 times that for the DC arc diamond deposition techniques on flat substrates.[33] There does not appear to be any other method presently proposed for producing CVD diamond sections at this rate. Furthermore, this analysis suggests that the increased diamond output should be achieved with no increase in the net gas flow or power consumption, which offers the prospect for more economical production of solid diamond shapes.

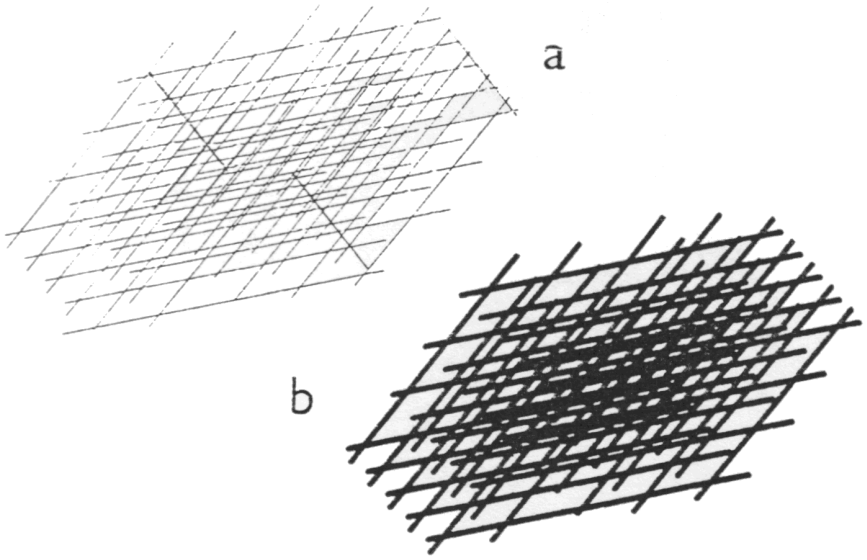

Fig. 22. Schematic diagram of a proposed 3-D fibre array (a) before and (b) after diamond deposition, illustrating the increased surface area, and hence growth rates that may be achieved.

7. Summary

The market for CVD diamond in various applications is predicted to exceed many hundreds of millions of dollars in the near future. However, the latest product form, diamond fibre with the diameter of human hair, may offer engineers, for the first time, the opportunity of exploiting diamond properties in large components and structures. These fibres may be embedded in thick or thin composite sections, with polymer, metallic or ceramic matrices, or be used to modify surface wear properties. We are still at the beginning of the learning curve for diamond fibre manufacture, but the potential and the challenge are now recognised.

Acknowledgments

The authors wish to thank the EPSRC and DRA (F) for financial support, Professors G.C. Allen, M.V. Lowson and J.W. Steeds, and Dr. N.M. Everitt for their support of the diamond programme, and K.N. Rosser, T. Baker, S.E. Johnson, R.J. Lade, J. Nicholson, S.A. Redman and J.D. Weeks for their many and varied experimental contributions to the work reported herein. PWM is grateful to the Royal Society for the award of a University Research Fellowship.

References

1) M. N. R. Ashfold, P. W. May, C. A. Rego and N. M. Everitt: Chem. Soc. Rev. **23** (1994) 21.
2) M. Seal: *Applications of Diamond Films and Related Materials*, NIST Special publication 885.

Eds. A. Feldman, Y. Tzeng, W. A. Yarbrough, M. Yoshikawa and M. Murakawa (NIST, 1995) p. 3.
3) C. J. H. Wort, J. R. Brandon, B. S. C. Dorn, J. A. Savage, R. S. Sussmann and A. J. Whitehead: *Applications of Diamond Films and Related Materials*, NIST Special publication 885, Eds. A. Feldman, Y. Tzeng, W. A. Yarbrough, M. Yoshikawa and M. Murakawa (NIST, 1995) p569.
4) M. D. Drory, R. J. McClelland, F. W. Zok, F. E. Heredia: J. Am. Ceram. Soc. **76** (1993) 1387.
5) P. W. May, C. A. Rego, R. M. Thomas, M. N. R. Ashfold, K. N. Rosser, P. G. Partridge, and N. M. Everitt: *Proc. 3rd Int. Symp. Diamond Mater.*, Honolulu, Hawaii, Proceedings Volume **PV 93-17**, Eds. J. P. Dismukes and K. V. Ravi (Electrochem. Soc., Pennington, NJ, 1993) p1036.
6) P. W. May, C. A. Rego, R. M. Thomas, M. N. R. Ashfold, K. N. Rosser, P. G. Partridge, N. M. Everitt: J. Mater. Sci. Lett. **13** (1994) 247.
7) A. A. Morrish, J. W. Glesener, M. Fehrenbacher, P. E. Pehrsson, B. Maruyama, P. M. Natishan: Diamond Relat. Mater. **3** (1993) 173.
8) P. G. Partridge, P. W. May, C. A. Rego, M. N. R. Ashfold: Mater. Sci. Technol. **10** (1994) 505.
9) E. D. Nicholson, J. E. Field, P. G. Partridge, M. N. R. Ashfold: Mat. Res. Soc. Symp. Proc. **383**, 101, Eds. M. D. Drory, D. B. Bogy, M. S. Donley, J. E. Field (MRS 1995).
10) J. Ting, M. L. Lake: J. Mater. Res. **9** (3) (1994).
11) J. Ting, M. L. Lake: J. Min. Met. Mater. Soc. **46** (1994) 23.
12) M. D. Drory, R. J. McClelland: Advan. Mater. (III-B) Conf., Tokyo, Japan, 1993, p869.
13) E. D. Nicholson, T. W. Baker, S. A. Redman, E. Kalaugher, K. N. Rosser, N. M. Everitt, M. N. R. Ashfold and P. G. Partridge: Diamond Relat. Mater. **5** (1996) 658.
14) P. G. Partridge, C. M. Ward-Close: Int. Mater. Rev. **38** (1993) 1.
15) B. Marayama, R. K. Everett, L. S. Cook, A. A. Morrish, P. Natishan, P. E. Pehrsson, A. E. Edelstein: *5th European Conf. on Comp. Mater.*, Bordeaux, France, April 1992, p715.
16) Reactor made by Thomas Swan and Co., Cambridge, UK.
17) P. W. May, C. A. Rego, M. N. R. Ashfold, K. N. Rosser, G. Lu, T. D. Walsh, L. Holt, N. M. Everitt and P. G. Partridge: Diamond Relat. Mater. **4** (1995) 794.
18) G. H. Lu, P. G. Partridge and P. W. May: J. Mater. Sci. Lett. **14** (1995) 1448.
19) P. G. Partridge, M. N. R. Ashfold, P. W. May and E. D. Nicholson: J. Mater. Sci. **30** (1995) 3973.
20) E. Kalaugher, Dept. of Aerospace Engineering, University of Bristol, unpublished work.
21) ASTM Designation C623-71, 229 (reapproved 1985).
22) S. Spinner, W. E. Tefft: Am. Soc. Test. Mater. Proc. **61** (1961) 1221.
23) D. H. Hughes: Br. Ceram Trans J. **87** (1988) 181.
24) ASTM Designation D3379-75 (reapproved 1989).
25) J. E. Emrick, H. L. Gegel: ASD Technical Report 61 – 168, Dec (1961).
26) D. S. Knight and W. B. White: J. Mater. Res. **4** (1989) 385.
27) Q. S. Chia, C. M. Younes, P. G. Partridge, G. C. Allen, P. W. May and C. A. Rego: J. Mater. Sci. **29** (1994) 6397.
28) V. G. Ralchenko, K. G. Korotushenko, A. A. Smolen, E. N. Loubnin: Diamond Relat. Mater. **4** (1995) 893.
29) H. Susiki, M. Yoshikawa, H. Tokura: *Adv. in New Diamond Science and Technology*, (MYU, Tokyo, 1994) p507.
30) K. V. Ravi, V. G. Zarifis: *Proc. 3rd Int. Symp. Diamond Mater.*, Honolulu, Hawaii, Proceedings Volume **PV 93-17**, Eds. J. P. Dismukes and K. V. Ravi (Electrochem. Soc., Pennington, NJ, 1993), 861.
31) V. N. Tokarev, J. J. B. Wilson, M. B. Jubber, P. John, D. K. Milne: Diamond Relat. Mater. **4** (1995) 169.
32) S. M. Pimenov, A. A. Smolin, V. G. Ralchenko, V. I. Konov, S. V. Likhanski, I. A. Veselovski, G. A. Sokolina, S. V. Bantsekov and B. V. Spitsyn: Diamond Relat. Mater. **2** (1993) 291.
33) J. V. Busch and J. P. Dismukes: Diamond Relat. Mater. **3** (1994) 295.